U. of Iowa 85-11

NASA CR-177835

Department of Physics and Astronomy

THE UNIVERSITY OF IOWA

Iowa City, Iowa 52242

GLOBAL AURORAL RESPONSES TO MAGNETOSPHERIC COMPRESSIONS BY SHOCKS IN THE SOLAR WIND: TWO CASE STUDIES

by

J. D. Craven[1], L. A. Frank[1], C. T. Russell[2]

E. J. Smith[3] and R. P. Lepping[4]

[1]Department of Physics and Astronomy
The University of Iowa
Iowa City, Iowa 52242

[2]Institute of Geophysics and Planetary Physics
University of California at Los Angeles
Los Angeles, California 90024

[3]Jet Propulsion Laboratory
California Institute of Technology
Pasadena, California 91109

[4]Laboratory for Extraterrestrial Physics
NASA/Goddard Space Flight Center
Greenbelt, Maryland 20771

April 1985

Department of Physics and Astronomy
The University of Iowa
Iowa City, Iowa 52242

ABSTRACT

Two case studies are presented of the global auroral responses to shocks in the solar wind at Earth. The z component of the interplanetary magnetic field, Bz, is negative ahead and behind the first shock and positive for the second case. A sudden-commencement geomagnetic storm develops in each case, with maximum $D_{st} \lesssim 190$ nT. An immediate auroral response is detected at all longitudes around the auroral oval, in which auroral luminosities increase by a factor of 2-3 with the first samples after each sudden commencement. The time delay in obtaining the first sample varies with local time from ~ 1 to 18 minutes. No other significant variations in the aurora are associated with the immediate response. Beginning ~ 30 minutes after each sudden commencement, the aurora becomes active and displays significant variations in its luminosity and spatial distribution. For $Bz < 0$ an intense substorm develops. A sun-aligned transpolar arc forms when $Bz > 0$, appearing first at local midnight as a polar arc and then lengthening sunward from the auroral oval across the polar cap to noon at an average speed of ~ 1 km/sec.

INTRODUCTION

Variations in solar-wind dynamic pressure and orientation of the interplanetary magnetic field (IMF) alter the magnitudes and distributions of currents around and within the magnetospheric cavity. One well-established signature of changes in these currents is an increase or decrease in the horizontal component of the magnetic field detected with magnetometers at low-latitude ground stations. For example, the magnetic field at all local times begins to increase abruptly, in $\lesssim$ 1 minute, in response to the collision of an interplanetary shock with the magnetosphere [e.g., Nishida, 1978]. The magnitudes of these increases are typically tens of nanoteslas. If no further changes occur in the solar wind or within the magnetosphere, the increase in field strength is identified as a sudden (positive) impulse. Of further significance is a rapid compression followed by a geomagnetic storm, in which the ring current undergoes a rapid (hours) main phase enhancement and auroral activity increases dramatically at higher latitudes. In this case, the low-latitude increase in the magnetic field is identified as the sudden commencement, or SC, of a geomagnetic storm. Unfortunately, the detection of changes in the surface magnetic field associated with interplanetary discontinuities can be ambiguous [e.g., Burlaga and Ogilvie, 1969], and a unique determination of the type of discontinuity can not be obtained from a clearly observed ground signature [e.g., Taylor, 1969; Chao and Lepping, 1974].

There is also an immediate response to a shock impact in the form of enhanced energetic (tens of keV) electron precipitation along the auroral oval. These increases are observed with riometers and balloon-borne x-ray detectors

[e.g., Brown et al., 1961; Matsushita, 1961; Ortner et al., 1962; Ullaland et al., 1970]. Increases in auroral luminosities are also reported [Vorob'yev, 1974]. The enhancements can begin simultaneously ($\lesssim$ 1 min) with SC onsets and last for ~ 3-10 minutes. The magnitudes of the enhancements vary from ~ 10% to factors of > 2, depending on the method of detection, and also vary from event to event. These immediate, brief increases are not associated with auroral substorms.

Many investigators have studied the response of the auroral electrojet to impacts by interplanetary discontinuities on the magnetosphere [Wilson and Sugiura, 1961; Kawasaki et al., 1971; Burch, 1972; Kokubun et al., 1977], with an emphasis on the triggering of auroral substorms. In brief summary, it appears that a substorm can be initiated following a shock impact for which the magnitude of the SC exceeds ~ 10 nT, and for which the IMF z-component, Bz, is negative for ~ 30 minutes before the SC [Burch, 1972]. However, the magnitude of the SC for triggering a substorm may depend on other parameters of the solar cycle [Kawasaki et al., 1971] and the amplitude of the IMF [Burch, 1972]. Extended periods of Bz positive prior to a SC will in general not lead to substorms [Burch, 1972]. Burch [1972] and Kokubun et al. [1977] interpret their observations to indicate that the state of the magnetosphere at the time of arrival of a shock is important in determining the magnetospheric response: pre-conditioning, such as in a growth phase, is important. Kokubun and colleagues conclude that substorm initiation remains an internal magnetospheric process accelerated by the shock-induced compression of the magnetosphere. In contrast, Akasofu and Chao [1980] argue that substorms which can follow shock impacts and SCs are the result of increases in the rate of direct energy transfer by the solar wind - magnetospheric dynamo. For no change in IMF

direction, the rate of energy transfer increases with increasing V and B across the shock. The more southward B, the greater the coupling and energy dissipation.

The maximum time delays from SCs to auroral substorm onsets used in the various investigations have not been identical. For example, Kawasaki et al. [1971] appear to use ± 3 minutes, while Kokubun et al. [1977] allow delays of up to 15 minutes in defining simultaneity. No unique relation is known for the time of substorm onset after a SC.

We wish to pursue further the auroral responses to the arrival of interplanetary shocks using time sequences of global auroral images routinely provided by the imaging photometers on board Dynamics Explorer 1 (DE 1) [Frank et al., 1981a]. Our objective is to monitor auroral luminosities prior to and following SCs for which the sign of Bz is the same on each side of the shock associated with the SC. For the first case, the IMF is directed well southward, and in the second case it is northward. In each case there is an immediate response followed in ~ 30 minutes by the onset of significant variations in luminosities and spatial distributions. For $Bz < 0$, an auroral substorm is observed. For the case of $Bz > 0$, sun-aligned, polar-cap auroral forms brighten, and a transpolar arc of a theta aurora is seen to develop initially at local midnight.

OBSERVATIONS

Magnetic Activity

The time histories of D_{st} and Kp [Solar-Geophysical Data, NOAA] for 20-22 October 1981 (Figure 1) reveal the presence of two small geomagnetic storms with peak D_{st} values $\lesssim$ 190 nT. The first storm is preceded by an 11-nT SC reported at 1309 UT on 20 October only by the Honolulu ground magnetometer. A rapid main-phase decrease follows in the surface magnetic field. Auroral activity in the three-hour interval from 1200 to 1500 UT which includes the SC is characterized by Kp = 7_-. The Kp values increase to 7_o in the next two three-hour intervals, and then decrease with the recovery phase of the geomagnetic storm. As shown in Figure 2a, the AE index is > 300 nT after 0600 UT, and after ~ 1100 UT semi-periodic, large increases to $\gtrsim$ 1000 nT are detected at ~ two-hour intervals until ~ 2000 UT. It will be shown in the next section that the IMF is predominantly southward for this event (See Figure 3). The downward direction of the arrow locating the SC at 1309 UT in Figure 1 denotes this predominant direction.

The second geomagnetic storm is preceded by a significant SC detected at more than 16 stations on 22 October 1981 (see Figure 1). Mean onset time for the SC is 0524:45 UT. A maximum SC amplitude of 88 nT is reported by Toolangi (magnetic latitude of -46.7°) for the horizonal component of the magnetic field. At Honolulu the reported amplitude is 22 nT. The Kp index is 4_o from 0300 to 0900 UT, and then increases with the delayed onset of the main-phase decrease. Maximum Kp values of 7_o are reached, identical to those for the earlier storm. The AE index is $\lesssim$ 125 nT in the 4 hours before the SC, and

increases to ~ 190 nT for ~ 2 hours after the SC (see Figure 2b). A brief (~ 3 min) increase to ~ 360 nT is initiated within one minute of the SC. Significant magnetic activity with AE > 1000 nT is present after ~ 1000 UT, at about the same time that the main-phase decrease develops. It will be shown that the IMF is predominantly northward for this event (see Figure 5). The upward direction of the arrow locating the SC at 0525 UT in Figure 1 denotes this predominant direction.

Event of 20 October

Observations with the ISEE-1 and -3 spacecraft demonstrate that Bz is predominantly negative for more than 12 hours prior to and for more than 6 hours after the SC of 20 October 1981. A portion of these observations with ISEE 1 is presented in Figure 3 for the period 0920-1440 UT to show that $|Bz| \sim B$ in the several hours prior to arrival of the solar-wind discontinuity at ~ 1300 UT, and that Bz is large and negative after passage of the discontinuity. Geocentric solar magnetospheric (GSM) coordinates are used. The time history of ground magnetic activity described previously is in full accord with these variations in B and Bz. Two points of note which make this a less than ideal case study for $Bz < 0$ are (1) the brief, ~ 10 minute, depression in B and concomitant rotation in IMF direction beginning at ~ 1258 UT, during which Bz is positive, and (2) the slow, ~ 10 minute, ramp in magnitude from ~ 6 nT to ~ 18 nT after 1305 UT. The IMF direction returns southward at ~ 1307 UT.

Analysis of the solar-wind plasma for the time interval around 1300 UT reveals abrupt increases in bulk speed, density and temperature at 1305:30 UT (± 30 sec), coincident with the initial rapid increase in the magnitude of the IMF. The bulk flow speed and ion temperature increase from ~ 600 km/sec and ~ 2×10^5 K to ~ 660 km/sec and ~ 3×10^5 K, respectively, and the relative

density increases by a factor of ~ 1.6 (J. T. Gosling, private communication). We identify the discontinuity at 1305 UT as an interplanetary shock, which when detected at ISEE 1 is embedded within a weaker solar-wind discontinuity for which the most prominant signature is a rotation of the IMF direction. The ~ 3.5-minute delay between detection of the shock with ISEE 1 at GSM coordinates (20.5, -7.5, -0.10 R_E) and the SC at Honolulu is consistent with the ~ 660 km/sec (6.2 R_E/min) speed of the shock in the solar wind, for a radially directed shock normal, and the greater Alfven speeds of propagation within the magnetosphere.

Auroral imaging of northern polar latitudes in the time intervals 0226-0718, 0917-1054 and 1200-1425 UT on 20 October 1981 shows that auroral activity is also consistent with the time history of AE in this period of Bz < 0. The 12 vacuum-ultraviolet (VUV) images of the latter time interval are presented in Plate 1 using a false-color format in which weaker luminosities of several kilorayleighs (kR) are coded in red and the greater luminosities of the active aurora and from the sunlit hemisphere (~ 20 kR) are coded gold to yellow. Below each image is the UT for the beginning of the 12-minute telemetering period for the image. During this observing period, the VUV-wavelength photometer operates in a mode for which an image is obtained with one filter and the next image is scanned with a companion filter of different passband. The two-filter sequence repeats cyclically. The first image, at upper left in the plate, has been gained using a passband which extends from 120 to 155 nm. Above Earth's limb, the photometer responds solely to solar Lyman-α radiation resonantly scattered by exospheric hydrogen [Rairden et al., 1983]. At auroral latitudes the principal emissions are due to atomic oxygen (OI) at 130.4 and 135.6 nm. The passband for the second image is 123-155 nm,

which removes contributions to the photometer response by Lyman-α radiation while maintaining high sensitivity to emissions from OI. Slightly reduced apparent brightness of the sunlit hemisphere for images of the first and fourth columns in the plate arises from the photographic processing.

During the 66-minute break in telemetry from 1054 to 1200 UT an auroral substorm onset and associated expansion are detected by ground magnetometers, beginning at ~ 1100 UT. Maximum AE ≈ 900 nT is recorded at 1200 UT as imaging is resumed. The first images of Plate 1 record the late recovery phase of this substorm. A discrete auroral form is clearly visible in the evening-to-midnight sector at the poleward edge of the auroral oval, and weaker, more diffuse auroral distributions are observed to extend around the auroral oval at lower latitudes in the night sector. Auroral luminosities are enhanced at the latitude of the polar cusp in the local-noon sector.

Careful comparisons of the first six images (1200 to 1313 UT) with the next two images (1313 to 1337 UT) show that auroral luminosities are greater around the auroral oval after the SC at 1309 UT (see frame at 1313 UT). This increase is seen more clearly in Figure 4a, where maximum absolute intensities are plotted for the local noon, dusk and midnight sectors as a function of the sample time at each local time. In the dusk sector, these maxima in emissions arise from the discrete auroral forms at the poleward edge of the auroral oval while at local midnight the emissions arise from diffuse emissions at more equatorward latitudes. Contributions from solar Lyman-α radiation and day-glow have been removed in determining the absolute luminosities. Prior to 1308 UT, luminosities around the oval vary between ~ 3 and 6 kR. The last sample at local noon (at 1308 UT) before the SC does not indicate an increase in luminosities. One minute later, at 1309 UT, samples in the dusk sector

provide the first indication of an auroral response, with luminosities increasing from ~ 3.5 to 6 kR. From 1317-1335 UT luminosities of ~ 8.5-12 kR are observed in the dusk and midnight sectors. At local noon, luminosities increase to ~ 20 kR before the polar cusp blends into the dayglow near the limb. We refer to this increase as the immediate auroral response to magnetospheric compression. With the ninth image of the sequence in Plate 1, beginning at 1337 UT, an intense and rapidly developing substorm appears near the equatorward edge of the oval at midnight. Maximum luminosities exceed 40 kR. The brief 500-nT increase in AE after 1330 UT (Figure 2a) is associated with the expansive phase of this substorm.

Event of 22 October

Observations of the IMF prior to and during the onset of the geomagnetic storm on 22 October 1981 are complicated by the absence of ISEE-1 measurements before the SC and a gap in telemetry from ISEE 3 during passage of the discontinuity. Direct observations near Earth coincident with the SC are available with IMP 8, but again, telemetry is brief in duration. Observations of the IMF available in the period 0215 through 0750 UT are presented in Figure 5. Telemetry transmission times (UT) are given for ISEE 1 and IMP 8. For ISEE 3, times are advanced by 36 minutes as determined by matching time profiles of the magnetic components of ISEEs 1 and 3 after ISEE 1 re-enters the solar wind at ~ 0640 UT. Using this time base, Bz turns northward at ~ 2354 UT on 21 October, more than 5 hours before the SC. The leading edge of the solar-wind discontinuity is detected with the IMP-8 magnetometer at 0528 UT, which is ~ 3 minutes after onset of the SC. The magnetic field turns southward after ~ 0830 UT, and is followed by the onset of the main-phase decrease for

the geomagnetic storm and increasing values for Kp in the next two 3-hour intervals (Figure 1). The amplitude of AE begins to increase after ~ 0800 UT in response to the decreasing positive amplitude of the Bz component of the IMF (see Figure 2b).

Plasma parameters for the solar wind measured on either side of the discontinuity are consistent with an identification of the discontinuity as a shock: bulk velocity increases from 455 to 575 km/s, ion density from 5.5 to ~ 14 cm^{-3} and ion temperature from ~ 5.5 × 10^4 to ~ 3.0 × 10^5 K (A. J. Lazarus, private communication). The solar-wind speed of 575 km/s behind the shock and a distance of 198 R_E to ISEE 3 within ~ 6° of the sun-earth line yields a time delay of 37 minutes, in agreement with that determined above. In the slower solar wind ahead of the shock, the time delay for radial propagation is 46 minutes. The approximate 3-minute delay between SC onset and detection of the shock at IMP 8 is believed to be due in part to the orientation of the shock normal relative to the location of the spacecraft at GSM coordinates (-2.4, 22.8, -30.8 R_E). Using averages of the IMF magnetic field measurements obtained just before and after the shock, and applying the coplanarity theorem, the shock normal direction is (-0.937, 0.293, -0.192) in GSM coordinates: the shock normal is oriented ~ 10° downward and ~ 20° toward dusk away from the antisolar direction. The angle between the shock normal and geocentric spacecraft position is 67°. Hence, the shock interacts with the magnetospheric cavity before reaching the spacecraft on the leeward side of the magnetospheric cavity. The greater propagation speeds for compressional waves in the magnetosphere (~1000 km/s) advance the arrival time of the SC relative to the arrival time of the shock at IMP 8.

Auroral images for the period 0237-0525 UT confirm the absence of any important auroral activity in the extended period of Bz > 0, and show that the

emissions are uniform and weak around the auroral oval. The last five images in this time interval and the next seven images for 0525 through 0651 UT are displayed in Plate 2, in a format identical to that of Plate 1. Auroral luminosities at local noon and midnight, and averages of luminosities in the dawn-dusk plane of the oval are presented in Figure 4b. Before the SC at 0525 UT, maximum luminosities are 1.5 to 3 kR. The immediate auroral response to the rapid magnetospheric compression is clearly visible in the sixth image of Plate 1, beginning at 0525 UT, and in Figure 4b by the step-like increase in luminosities to ~ 5 to 8 kR at all local times. About 30-minutes later the aurora brightens at midnight and a sun-aligned polar arc begins to form at midnight. The sun-aligned polar arc then lengthens across the polar cap to local noon at an average speed of ~ 1 km/sec. No significant increases are observed in the magnitude of the AE index during this period of arc formation following the SC (Figure 2b).

The lack of measurements in the interplanetary medium from ~ 0535 to 0620 UT prohibits the identification of variations in the IMF which may be causally related to this unusual formation of a transpolar arc of the theta aurora. However, the continuing presence of relatively bright, sun-aligned auroral forms within the polar cap throughout the interval of the gap in telemetry is consistent with Bz remaining positive. A southward turning of the IMF is expected to cause a decrease in luminosities within the polar cap [Frank et al., 1985].

DISCUSSION

Two case studies of the auroral responses to magnetospheric compressions by shocks in the solar wind identify an immediate response within 1-10 minutes of the SC. This response is independent of the sign of Bz and is observed at all local times around the auroral oval. There seems little doubt that this global reponse is related to the 'direct' auroral response observed from the ground over a wide range of longitudes by Vorob'yev [1974] within $\lesssim$ 2 minutes of SCs. However, durations and amplitudes for the increases in auroral luminosities observed by Vorob'yev are ~ 3-8 minutes and ~ 25%, respectively. This short duration is similar to the duration of initial responses to SCs observed in auroral x-rays and with riometers [e.g., Brown et al., 1961; Matsushita, 1961; Ortner et al., 1962; Ullaland et al., 1970], and to the ~ 3-minute, ~ 230-nT increase in AE observed here for the SC of 22 October 1981 (Bz > 0 case). In contrast, the immediate auroral responses presented here are increases by factors $\gtrsim$ 2 in auroral luminosities over durations of greater than 10-20 minutes (Bz > 0). For the case of Bz < 0, no decrease in luminosities is observed before substorm onset (see Figure 4a). We have not investigated here, using simultaneous auroral observations with DE at visible wavelengths, any dependence of the immediate auroral response on the energy of the precipitating electrons.

The amplitude-time profile for the immediate auroral response is probably related to the speed and orientation of the IMF discontinuity and the magnitude of the increase in solar-wind momentum flux. For example, at 600 km/sec (5.6 R_E/min), a discontinuity propagating in the antisunward direction will envelop the magnetosphere from X = 10 to -30 R_E in ~ 7 minutes. Faster prop-

agation at non-radial orientations may speed the global onset and shorten the interaction time. For the relatively slow shocks discussed here, the higher Alfven speeds within the magnetospheric cavity (~1000 km/s) may also influence the onset times for magnetic and auroral activity. The increases in solar-wind momentum flux for the two shocks are by factors of 1.8 ($B_z < 0$ on 20 October) and 4.1 ($B_z > 0$ on 22 October). The second, larger increase is associated with the more widely reported SC of greater amplitude.

While the latitudinal response of the auroral emissions has not been studied here quantitatively, the auroral images show that the pre-existing discrete and diffuse auroral forms both brighten after the SC. Surveys of the DE-1 auroral images and the IMP-8 and ISEE-1 and -3 measurements of the IMF show that the immediate increases in auroral luminosities around the auroral oval are routinely detected in association with abrupt increases in IMF magnitude. Auroras in the local-noon sector appear to be particularly sensitive. We conclude that plasmas of the magnetopause boundary layer, and the dayside and outer magnetosphere are affected by the rapid magnetospheric compression that stimulates increased particle precipitation. Future analysis may determine the relative importance of increases in IMF magnitude and solar-wind momentum flux in determining the amplitude of the immediate increase in auroral luminosities.

For the case of Bz > 0, the immediate response is more striking than for Bz < 0 due to the lower emission rates before the SC. The later, delayed onset of a localized brightening at midnight followed by the ~ 1 km/sec sunward lengthening of a sun-aligned, polar arc of the theta aurora has only one counterpart in the DE data base of auroral images reviewed to date. However, the other example of sunward lengthening of a polar arc from the oval near mid-

night occurs in a period of apparent quiescent conditions in the solar wind. The IMF Bz component is positive. These observations suggest that in response to magnetospheric compressions for which Bz > 0, plasma flows in the plasma-sheet boundary layer can be directed out of the plane of the geomagnetic tail and into the tail lobes. The direction of plasma flow and width of this plasma region would be guided and determined by pre-existing sunward flow patterns established during the lengthy period of Bz > 0 [Maezawa, 1976; Burke et al., 1979; 1982]. The magnetospheric response time observed here is ~ 30 minutes for the onset of initial or enhanced plasma flow normal to the plane of the plasma sheet.

Research cited earlier is concerned with the triggering of substorms by shocks, where the substorm onsets occur no later than 15 minutes after the shock-induced SC onsets. From this earlier work it is seen that under certain favorable conditions a substorm onset, as determined by ground magnetometers, can occur within minutes of the shock impact. For the case of Bz < 0 studied here, these favorable conditions are not present.

We note from Figures 1 and 2 that the maximum amplitudes and overall temporal variations of the auroral and ring-current indices are very similar for the two geomagnetic-storm periods, where the storm of 22 October begins only after the IMF turns southward ~ 3 hours after the shock crossing. We conclude that the gross energetics of the storm periods are similar, and that the only signficant variable which differentiates physical conditions external to the magnetosphere for the two cases is the sign of Bz. In each case, significant auroral activity begins within ~ 30 minutes of the SC. For the case of Bz < 0 an auroral substorm is observed along the oval in the midnight sector. For the case of Bz > 0, the dynamic evaluation of the aurora takes place within

the polar cap: a polar substorm. The sunward edge of the lengthening polar arc represents, for the polar substorm, an analog to the westward-traveling surge of an auroral-oval substorm. The 1-km/sec speed of the sunward-traveling surge is typical of westward-traveling surges which travel along the pre-existing discrete auroral forms. This suggests that faint, discrete, sun-aligned auroral forms undetected with DE 1 may have been present within the polar cap in advance of the shock impact as part of the established polar-cap convection pattern.

We conclude that the ~ 30-minute time delay in the onset of auroral activity is independent of the sign of Bz and is related to the time constant for reconfiguration of the geomagnetic tail in response to changes in the IMF and solar-wind plasma behind the shock. In the solar wind, the shocks of 20 and 22 October travel to $X \simeq -186$ and -162 R_E, respectively, in 30 minutes. As typical Alfven speeds within the plasma sheet and its boundary layer ($n \sim 0.1 - 1$ cm^{-3}, $B \sim 25$ nT; $V_A \sim 545 - 1723$ km/s) are similar to or greater than the speeds of these relatively slow shocks (~ 660 and 575 km/sec), the compressional waves will travel at least as far down the geomagnetic tail in 30 minutes. Propagation speeds within the tail lobes exceed those in the plasma sheet. If a localized critical region within the geomagnetic tail is dominant in controlling the substorm process, then the time from first signal arrival to substorm onset may be a measure of the time required for reconfiguration of the geomagnetic tail.

For the plasmoid model of Hones [e.g., Hones, 1984] the critical-region distance is $X \sim -15$ R_E, so > 25 minutes are available for the reconfiguration. For a model of magnetotail dynamics which emphasizes the plasma-sheet boundary layer [Frank et al., 1981b; Eastman et al., 1984] and a more distant

acceleration region associated by Williams [1981] with energetic ions in the plasma-sheet boundary layer, the distance is $X \sim -100\ R_E$ and the available time for reconfiguration is > 10 minutes.

ACKNOWLEDGEMENTS

The AE data have been kindly provided through the efforts of Dr. S.-I. Akasofu at the University of Alaska. We wish to thank Dr. A. J. Lazarus of the Massachusetts Institute of Technology and Dr. J. T. Gosling of the Los Alamos National Laboratory for analyzing and providing solar-wind plasma parameters associated with the shocks. This research at the University of Iowa has been supported in part by the National Aeronautics and Space Administration under contract NAS5-25689 and grants NGL-16-001-002 and NAG5-483, and by the Office of Naval Research under grant N00014-76-C-0016. At the University of California at Los Angeles this research has been supported by the National Aeronautics and Space Administration under contract NAS5-28448. The research conducted at the Jet Propulsion Laboratory of the California Institute of Technology was carried out under contract to the National Aeronautics and Space Administration.

REFERENCES

Akasofu, S.-I., and J. K. Chao, Interplanetary shock waves and magnetospheric substorms, Planet. Space Sci., 28, 381-385, 1980.

Brown, R. R., T. R. Hartz, B. Landmark, H. Leinbach and J. Ortner, Large-scale electron bombardment of the atmosphere at the sudden commencement of a geomagnetic storm, J. Geophys. Res., 66, 1035-1041, 1961.

Burch, J. L., Preconditions for the triggering of polar magnetic substorms by storm sudden commencements, J. Geophys. Res., 77, 5629-5632, 1972.

Burke, W. J., M. C. Kelley, R. C. Sagalyn, M. Smiddy and S. T. Lai, Polar cap electric field structures with a northward interplanetary magnetic field, Geophys. Res. Lett., 6, 21-24, 1979.

Burke, W. J., M. S. Gussenhoven, M. C. Kelley, D. A. Hardy and F. J. Rich, Electric and magnetic field characteristics of discrete arcs in the polar cap, J. Geophys. Res., 87, 2431-2443, 1982.

Burlaga, L. F., and K.W. Ogilvie, Causes of sudden commencements and sudden impulses, J. Geophys. Res., 74, 2815-2825, 1969.

Chao, J. K., and R. P. Lepping, A correlative study of SSC's, interplanetary shocks, and solar activity, J. Geophys. Res., 79, 1799-1807, 1974.

Eastman, T. E., L. A. Frank, W. K. Peterson and W. Lennartsson, The plasma sheet boundary layer, J. Geophys. Res., 89, 1553-1572, 1984.

Frank, L. A., J. D. Craven, K. L. Ackerson, M. R. English, R. H. Eather and R. L. Carovillano, Global auroral imaging instrumentation for the Dynamics Explorer mission, Sp. Sci. Instr., 5, 369-393, 1981a.

Frank, L. A., R. L. McPherron, R. J. DeCoster, B. G. Burek, K. L. Ackerson and C. T. Russell, Field-aligned currents in the earth's magnetotail, J. Geophys. Res., 86, 687-700, 1981b.

Frank, L. A., J. D. Craven and R. L. Rairden, Images of the earth's aurora and geocorona from the Dynamics Explorer mission, Adv. Space Res., (in press), 1985.

Hones, E. W., Jr., Plasma sheet behavior during substorms, Magnetic Reconnection in Space and Laboratory Plasmas, ed. by E. W. Hones, Jr., AGU Geophys. Monograph No. 30, p. 178, 1984.

Kawasaki, K., S.-I. Akasofu, F. Yasuhara and C.-I. Meng, Storm sudden commencements and polar magnetic substorms, J. Geophys. Res., 76, 6781-6789, 1971.

Kokubun, S., R. L. McPherron and C. T. Russell, Triggering of substorms by solar wind discontinuities, J. Geophys. Res., 82, 76-86, 1977.

Maezawa, K., Magnetospheric convection induced by the positive and negative Z components of the interplanetary magnetic field: quantitative analysis using polar cap magnetic records, J. Geophys. Res., 81, 2289-2303, 1976.

Matsushita, S., Increase of ionization associated with geomagnetic sudden commencements, J. Geophys. Res., 66, 3958-3961, 1961.

Nishida, A., Geomagnetic Diagnosis of the Magnetosphere, Springer-Verlag, New York, 1978.

Ortner, J., B. Hultqvist, R. R. Brown, T. R. Hartz, O. Holt, B. Landmark, J. L. Hook and H. Leinbach, Cosmic noise absorption accompanying geomagnetic storm sudden commencements, J. Geophys. Res., 67, 4169-4186, 1962.

Rairden, R. L., L. A. Frank and J. D. Craven, Geocoronal imaging with Dynamics Explorer: A first look, Geophys. Res. Lett., 10, 533-536, 1983.

Taylor, H. E., Sudden commencement associated discontinuities in the interplanetary magnetic field observed by IMP 3, Solar Phys., 6, 320-334, 1969.

Ullaland, S. L., K. Wilhelm, J. Kanges and W. Riedler, Electron precipitation associated with a sudden commencement of a geomagnetic storm, J. Atmos. and Terr. Phys., 32, 1545-1553, 1970.

Vorob'yev, V. G., Sc-associated effects in auroras, Geomagn. Aeron., 14, 72-74, 1974.

Williams, D. J., Energetic ion beams at the edge of the plasma sheet: ISEE 1 observations plus a simple explanatory model, J. Geophys. Res., 86, 5507-5518, 1981.

Wilson, C. R., and M. Sugiura, Hydromagnetic interpretation of sudden commencements of magnetic storms, J. Geophys. Res., 66, 4097-4111, 1961.

PLATE CAPTIONS

Plate 1. Sequence of 12 consecutive false-color auroral images at ultraviolet wavelengths in the time interval 1200 through 1425 UT on 20 October 1981. Below each image is the UT for the beginning of the 12-minute telemetering period for the image. Increased luminosities following the SC at 1309 UT are seen with the seventh image at 1313 UT. Substorm onset is first detected with the ninth image at 1337 UT. Predominant direction of the IMF Bz component is southward. See the text for a discussion of ultraviolet filters used.

Plate 2. Continuation of Plate 1 for the time interval 0417 through 0650 UT on 22 October 1981. The SC occurs at 0525 UT with the beginning of the sixth frame. Predominant direction of the IMF Bz component is northward.

FIGURE CAPTIONS

Figure 1. Hourly averages of D_{st} and the three-hour values of Kp for 20-22 October 1981. The onset time for each sudden commencement (SC) of interest here is identified.

Figure 2. (a) The AE index for 20 October 1985. (b) The AE index for 22 October 1985. Times for the SCs of interest here are identified.

Figure 3. Magnitude of the IMF and its components in GSM coordinates as observed with ISEE 1 on 20 October 1981 from 0920 to 1440 UT.

Figure 4. (a) Maximum emission intensities of atomic oxygen at 130.4 and 135.6 nm along the auroral oval in the noon, dusk and midnight sectors for the ~ 2-hour time interval surrounding the SC at 1309 UT on 20 October 1981. (b) Continuation of Figure 4a for 22 October 1981 and the SC at 0525 UT. Averages are given for the intensities in the dawn and dusk sectors.

Figure 5. Continuation of Figure 3 for 22 October 1981 from 0215 to 0750 UT, using observations with ISEEs 1 and 3 and IMP 8. For ISEE 3, time is advanced by 36 minutes as determined by matching time profiles of the magnetic components of ISEEs 1 and 3 after ISEE 1 re-enters the solar wind at ~ 0640 UT.

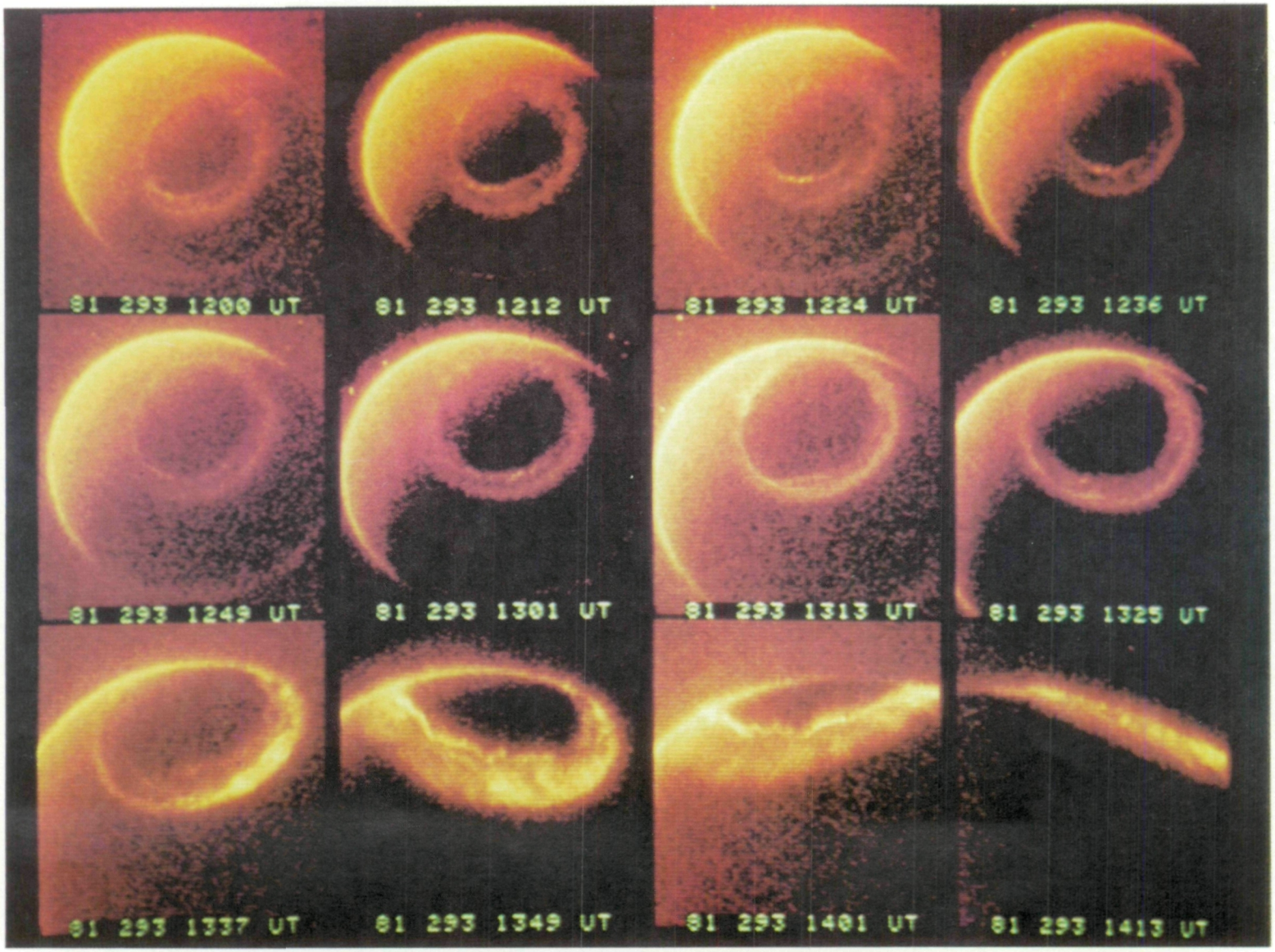

Plate 1

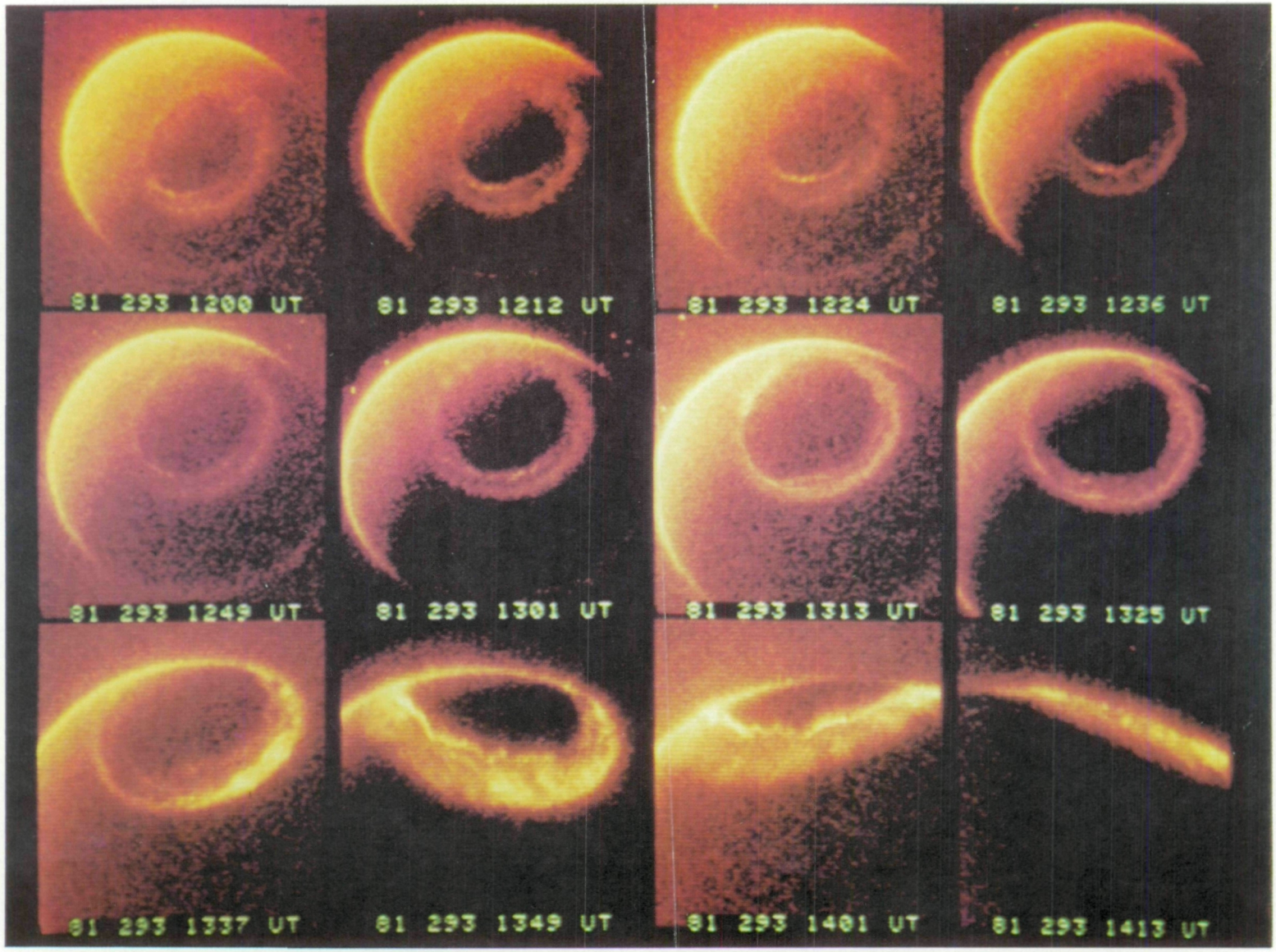
81 293 1200 UT
81 293 1212 UT
81 293 1224 UT
81 293 1236 UT
81 293 1249 UT
81 293 1301 UT
81 293 1313 UT
81 293 1325 UT
81 293 1337 UT
81 293 1349 UT
81 293 1401 UT
81 293 1413 UT

Plate 1

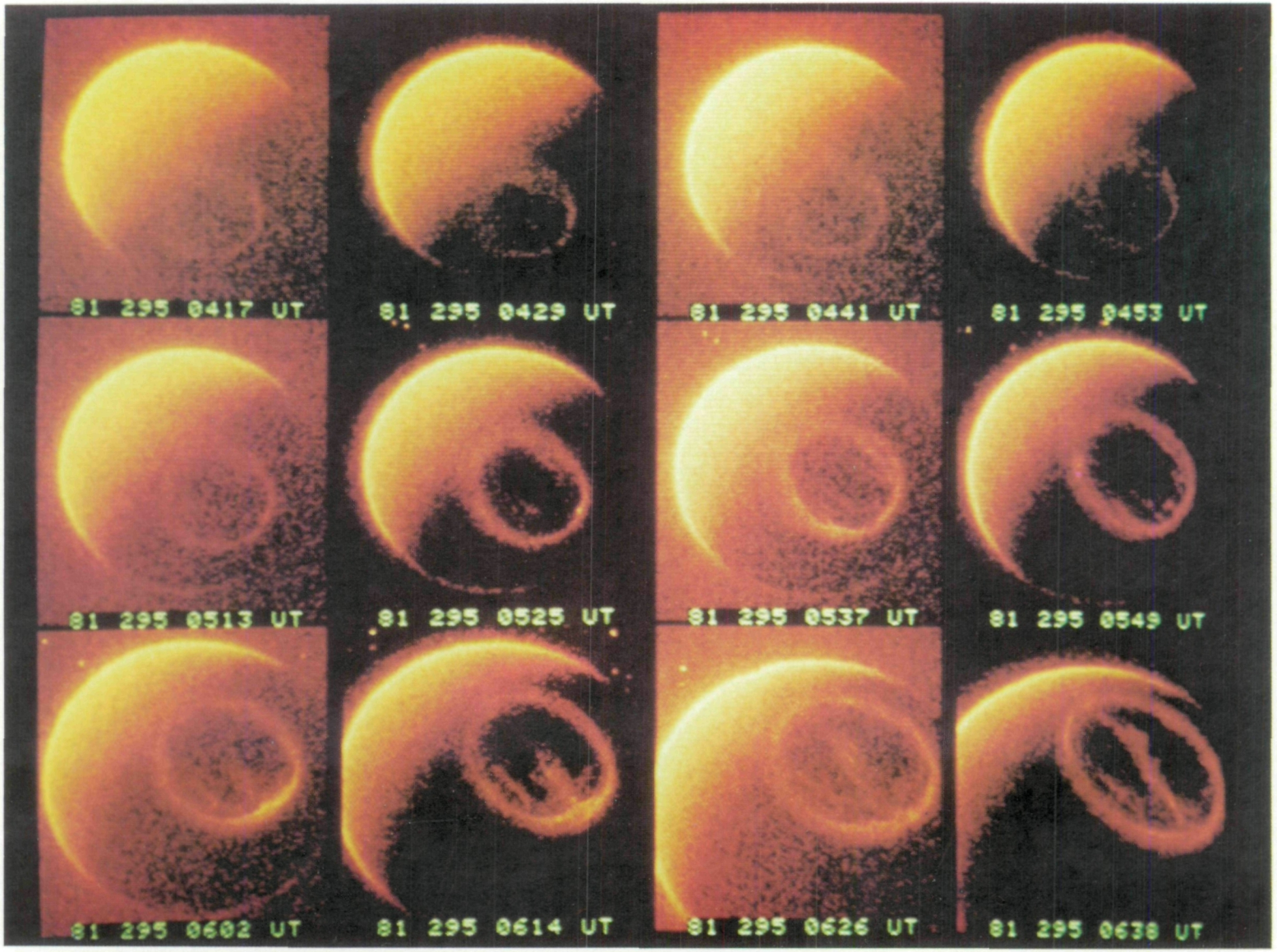

Plate 2

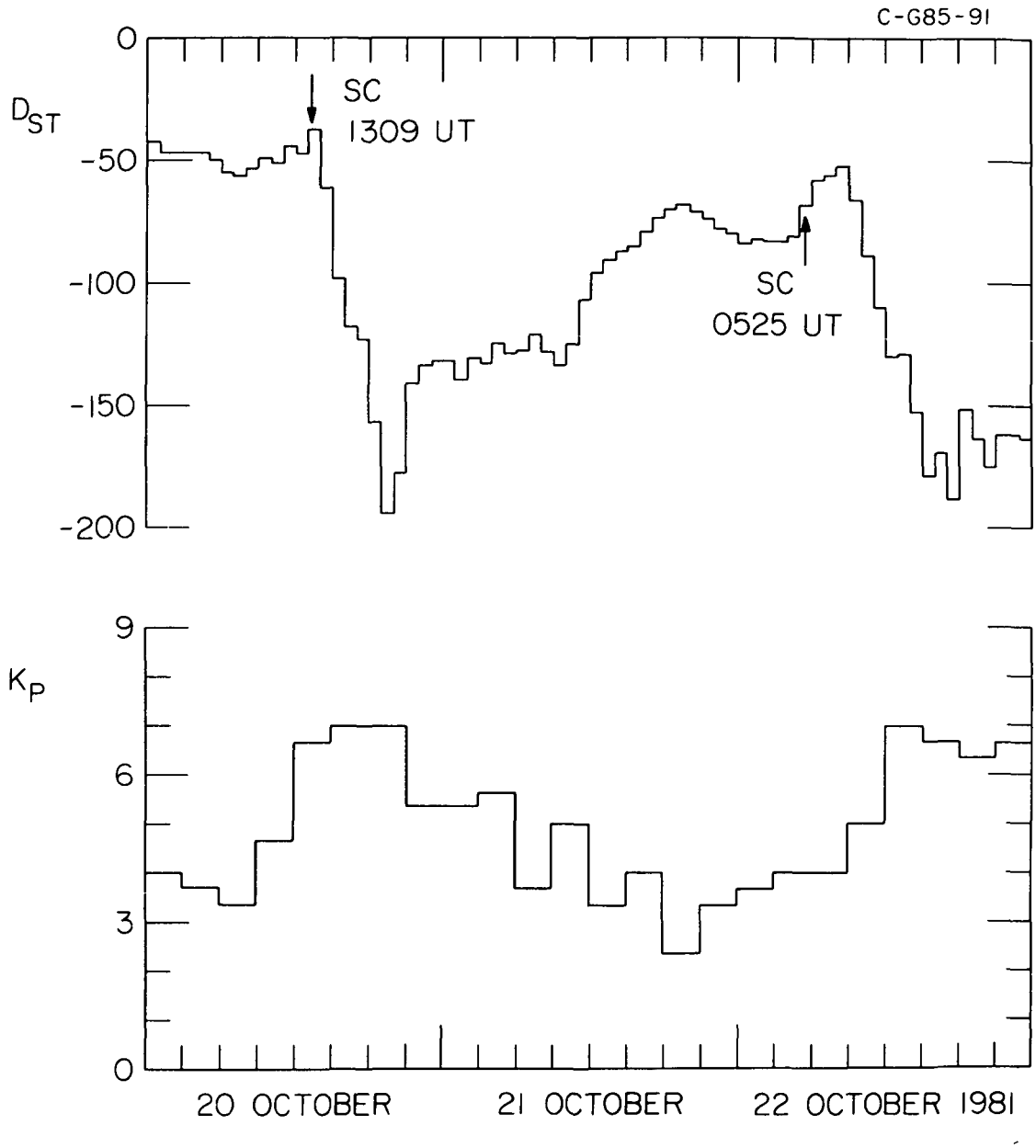
C-G85-91
0
-50
-100
-150
-200
D_{ST}
SC
1309 UT
SC
0525 UT
9
6
3
0
K_P
20 OCTOBER
21 OCTOBER
22 OCTOBER 1981

Figure 1

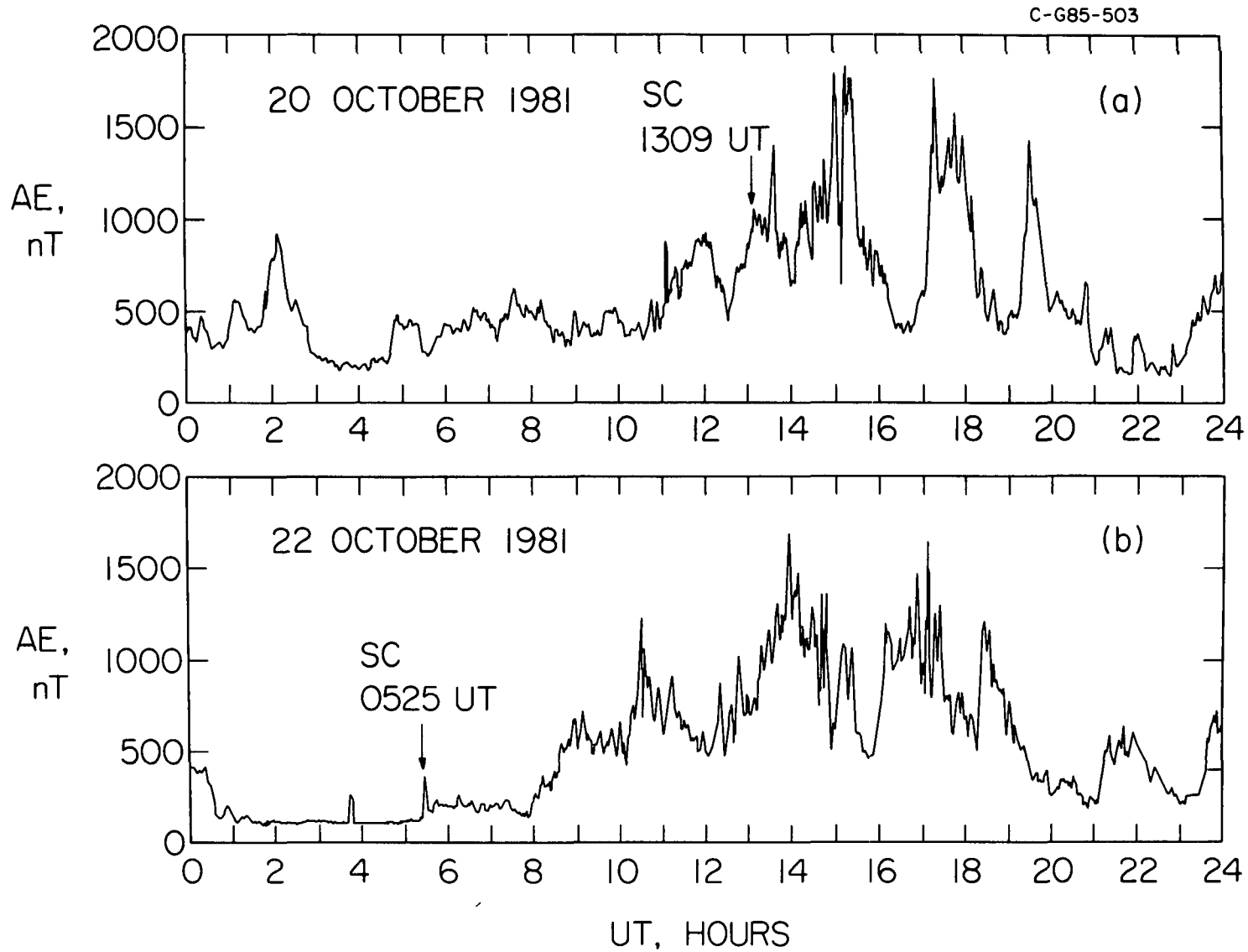
C-G85-503
20 OCTOBER 1981
SC
1309 UT
(a)
AE, nT
2000
1500
1000
500
0
0 2 4 6 8 10 12 14 16 18 20 22 24
22 OCTOBER 1981
SC
0525 UT
(b)
AE, nT
2000
1500
1000
500
0
0 2 4 6 8 10 12 14 16 18 20 22 24
UT, HOURS

Figure 2

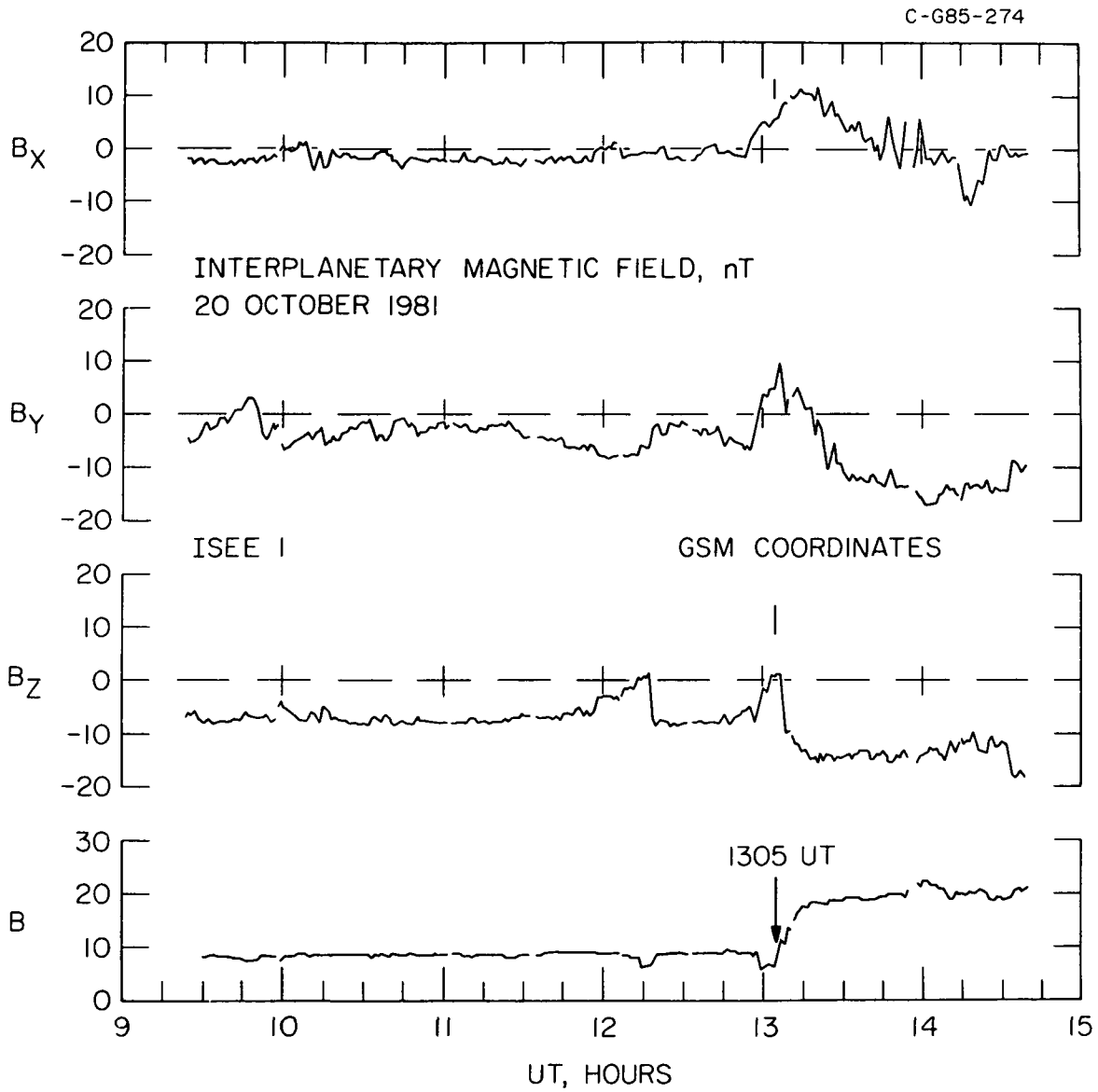
C-G85-274
INTERPLANETARY MAGNETIC FIELD, nT
20 OCTOBER 1981
ISEE 1
GSM COORDINATES
B_X
B_Y
B_Z
B
1305 UT
UT, HOURS

Figure 3

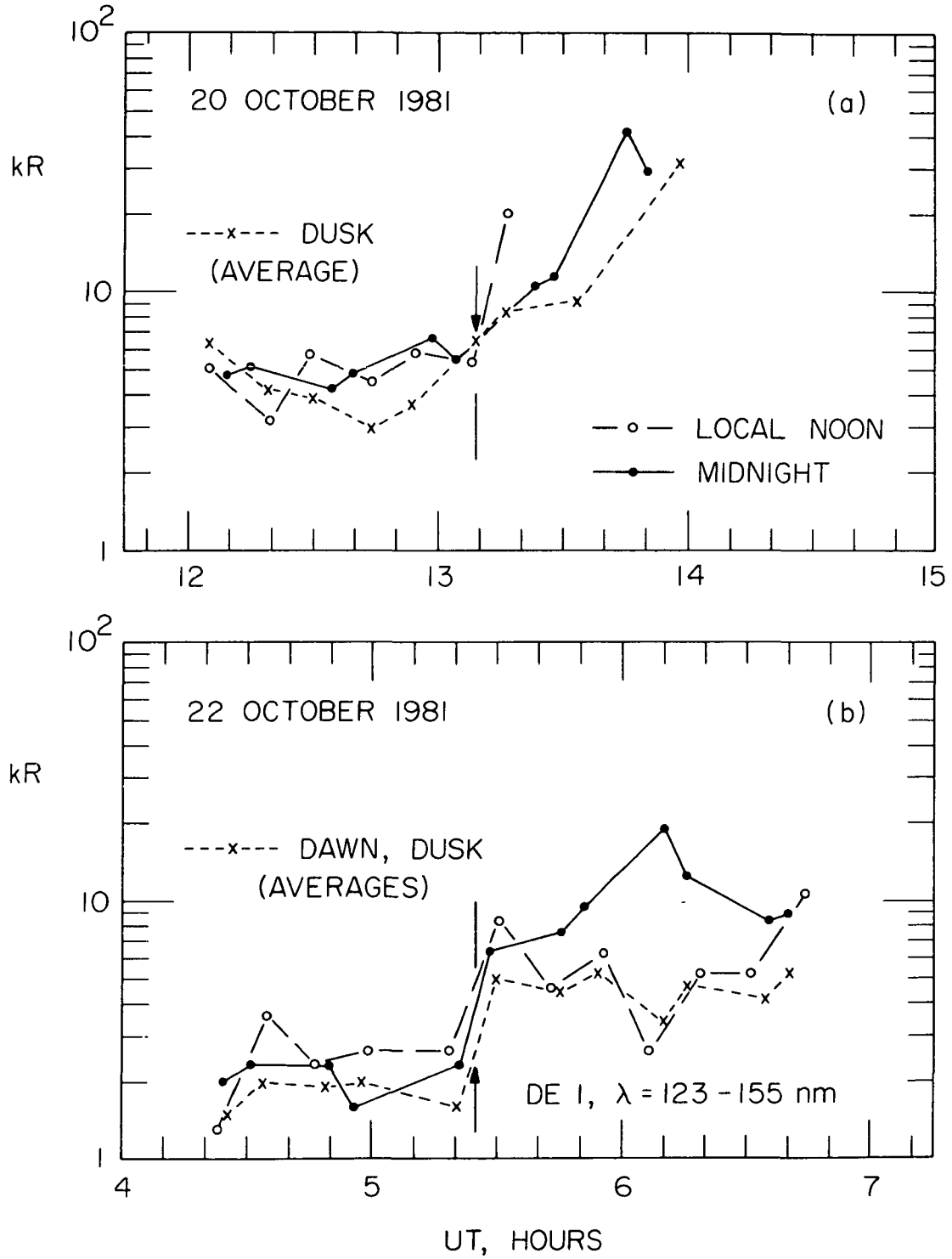
10^2
20 OCTOBER 1981
(a)
kR
---x--- DUSK
(AVERAGE)
10
—o— LOCAL NOON
—●— MIDNIGHT
1
12
13
14
15
10^2
22 OCTOBER 1981
(b)
kR
---x--- DAWN, DUSK
(AVERAGES)
10
DE 1, λ = 123 - 155 nm
1
4
5
6
7
UT, HOURS

Figure 4

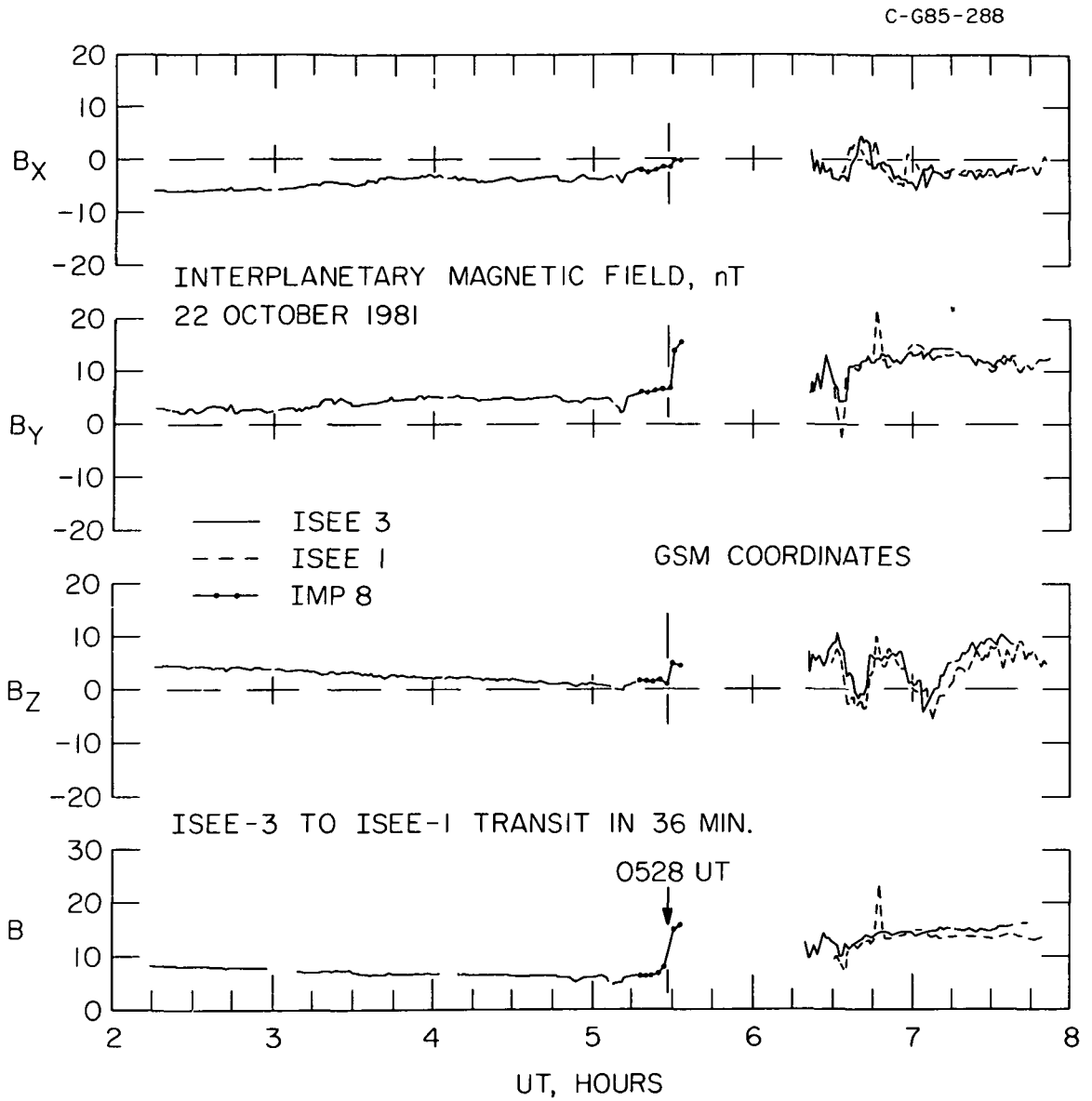
C-G85-288
INTERPLANETARY MAGNETIC FIELD, nT
22 OCTOBER 1981
ISEE 3
ISEE 1
IMP 8
GSM COORDINATES
ISEE-3 TO ISEE-1 TRANSIT IN 36 MIN.
0528 UT
B_X
B_Y
B_Z
B
UT, HOURS

Figure 5